An experimental study of machinability of FGH95 in end milling with coated carbide tools

DU Jin[a], LIU Zhanqiang[a], TANn Chao[b], PANG Jiyou[b]
[a]School of Mechanical Engineering, Shandong University, Jinan, Shandong China, 250061
[b]Shenyang Lining Aero-Engine Group Corporation, Shenyang, Liaoning,, China, 110043

ABSTRACT

FGH95 is one of difficult-to-cut nickel-based powder metallurgy (PM) superalloys which are commonly used in advanced turbo-engines. Firstly, this paper presents an orthogonal design experiments to study the cutting force and cutting temperature variations in the end milling of FGH95 with two kinds of coated carbide tools. It is found that AlTiN coated solid carbide end mill is suit for machining FGH95 nickel-based powder metallurgy superalloy. Experimental results show that with the increase of cutting speed, radial depth of cut, feed rate, there is a growing tendency in cutting forces. Among the cutting condition parameters, cutting speed has the greatest influence on cutting forces, especially when cutting speed exceeds 55m/min. With the increase of cutting speed and radial depth of cut, cutting temperature increases. However the cutting temperature decreases slightly as the increasing of feed rate. Reason for temperature variations is investigated in this paper. Secondly, tool wear mechanism in end milling of FGH95 is analyzed. It is shown that chipping on cutting edge is the most dominate wear mechanism which dominates the deterioration and final failure of the coated carbide tools. Thirdly, the machined surface topography is measured with white light interferometer and Super depth digital microscope. Based on the measurement, it is found that better surface roughness and waviness are obtained with using AlTiN coated carbide tools than by TiAlN/TiN/TiAlN coated ones.

Keywords: FGH95, superalloy, milling, cutting force, cutting temperature, tool wear

1. INTRODUCTION

Numerous investigators have dealt with the issue of cutting forces and cutting temperatures of machining nickel-based superalloy from both the experimental and analytical aspects. However, the research for machining nickel-based superalloy which product via PM routes is rare. Powder Metallurgy nickel-base superalloy such as FGH95 have been developed for turbine disk applications in advanced turbo-engines due to its homogeneous and fine grains provide high tensile properties [1-4]. Machining of advanced FGH95 superalloy is grim difficulties and challenges. This is due to a more complex combination of material properties, including lowering of thermal conductivity that leads to elevating temperatures at the tool/chip interface during cutting, work hardening tendency during machining that becomes more severe with increase strengthening of this kind of superalloy, and intensive adhesion to the surface of the tooling under operation [5-8]. PM superalloy porosity affects its mechanical properties and machinability. Porosity decreases the thermal conductivity of PM superalloy parts, high temperature leads to poor quality workpieces and generates concentrated thermal damage at the cutting edge of a tool[9~10]. Thermal phenomena plays a key role in the mechanics and machinability of PM superalloy[11]. On the contrary, porosity improves machinability due to the porosity generating interrupted cutting condition on a microscopic scale. The tool tip is continually impacted as it repeatedly moves from pore to solid particle, producing very small fatigue cracks and fine chips along the cutting edge. The individual particles that make up the component are often extremely hard, much harder than the overall part. Many PM superalloy parts undergo heat treatment to make them harder and stronger. Even while part bulk hardness measure HRC 40~45, the hardness of the individual particles that make up the part can reach HRC60. These hard particles cause severe and rapid

Fourth International Seminar on Modern Cutting and Measurement Engineering,
edited by Jiezhi Xin, Lianqing Zhu, Zhongyu Wang, Proc. of SPIE Vol. 7997,
799717 · © 2011 SPIE · CCC code: 0277-786X/11/$18 · doi: 10.1117/12.887465

edge wear [12]. Due to the presence of porosity and structure of sintered powder metallurgy superalloy, the machinability of such materials often bears a little resemblance to materials of similar composition of cast or wrought origin.

No porosity is expected to be present in hot isostatic pressed (HIP) PM superalloy. However, large amounts of hard oxide inclusions cause increased wear of tools due to an increased oxygen content[13].

New generation coated solid carbide end mill providing efficiency in milling operations are being developed and utilized for machining hard-to-cut high-strength superalloys. A set of experiments will be performed in this study to measure the cutting temperature and cutting force components in case of milling FGH95 nickel-based PM superalloy. The differences in machinability between machining FGH95 nickel-based PM superalloy with KC633M (TiAlN/TiN/TiAlN coated carbide tool) and KC643M (AlTiN coated carbide tool) will be studied to find cutting force and cutting temperature variously.

2. EXPERIMENTAL SETUP

2.1 Test materials

The workpiece materials are HIPed PM nickel-based superalloy FGH95. The chemical compositions of FGH95 are given in Tab.1. The microstructures of FGH95 after HIP and normal heat treatment is exhibited in Fig.1. There are primary dendrites and primary particle boundary (PPB), and the grain size is about ASTM 6-7. Defects in PM superalloy include PPB, TIP (thermally induced porosity) and nonmetallic inclusions [14], which are the crack sources that decrease stress rupture and tensile ductility, and make the machinability of FGH95 be worsen.

Table1: Chemical compositions of the studied FGH95 (wt.%)[15]

·C	Cr	Co	W	Mo	Al	Ti	Nb	Ni
0.060	12.98	8.00	3.40	3.40	3.48	2.55	3.50	Bal

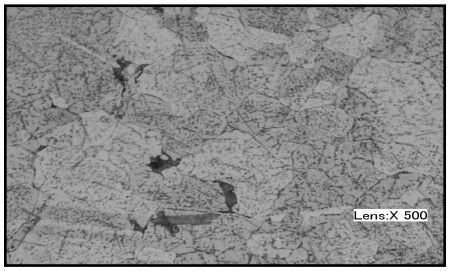

Figure 1: Microstructure of FGH95 after HIP

2.2 Machine tool

Machining tests were performed on a numerically controlled vertical milling machine DMU 70V with power 15kw, maximum rotation speed 18000rpm. A Kistler Type 9257B quartz three-component dynamometer was mounted on the machine table to measure the cutting force. The workpiece was mounted on the dynamometer though a specially designed fixture. A TH4105 portable thermal infrared imager was utilized to measure the cutting temperature.

Table2: Dimensions of two kinds of tool

	Number of flutes	d/mm	D/mm	L/mm	l/mm	Rε/mm	Helix angle
Tool A	4	12	11.5	84	18	3	38°
Tool B	5	12	12	84	26	3	38°

2.3 Cutting tool

The tools used were:

Tool A: TiAlN/TiN/TiAlN coated carbide end mill.

Tool B: AlTiN coated carbide end mill.

The geometry of coated solid carbide end mill is shown in Fig.2 and Tab.2.

2.4 Experimental parameters

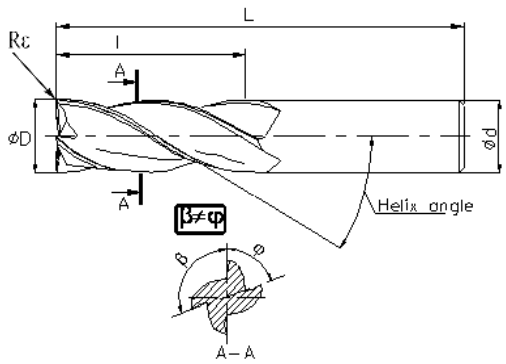

Figure 2: Sketches of tool geometry

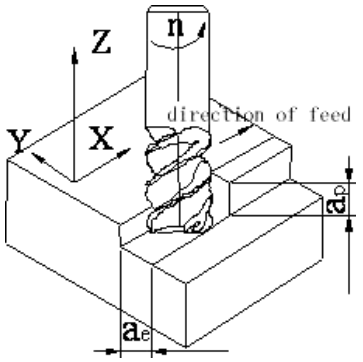

Figure 3: Schematic drawing of milling operations

The machining tests were carried out in end milling operations. The adopted cutting conditions are listed in Tab.3 (Width of cut a_e=9mm is constant). Fig.3 illustrates the machining process parameters. Tests were carried out in cutting on FGH95 workpieces. The different cutting parameters for tool A and tool B were chosen in order to exclude catastrophic failure. The machining tests were divided into two groups: milling with the tool A and milling with the tool B, respectively. In each group, three factor-three level orthogonal tests were carried out, so $L_9(3^4)$ orthogonal arrays were adopted. For each test the cutting force F and cutting temperature T were measured.

Table 3: Cutting conditions

Tool	A(KC633M)	B(KC643M)
Feed rate(f)(mm/z)	0.02-0.04-0.06	0.02-0.04-0.06
Cutting speed(v)(m/min)	25-35-45	45-55-65
Radial depth of cut (a_p)(mm)	0.3-0.6-0.9	0.3-0.6-0.9
Coolant	Dry	Dry

2.5 Cutting force in end milling

The cutting force components acting on one tooth of the end mill cutter are shown in Fig.3, where the table system of cutting forces is: *Fx*=feed cutting force component (the instantaneous cutting force in the X direction); *Fy*=radial cutting force component (the instantaneous cutting force in the Y direction); and *Fz*=axial cutting force component (the instantaneous cutting force in Z direction).

3. RESULTS AND DISCUSSIONS

3.1 Cutting force tests

The machining test of milling with tool A was interrupted due to the tool red-hot and rapid damage when cutting speed exceeds 35m/min. There was no data about cutting force and cutting temperature from serials from 7 to 9 for the milling tests with tool A. Under the same condition, tool B played a better performance than tool A in machining the FGH95 superalloy. From the test results, it was obvious that as the tests carried out cutting force grows rapidly when machining FGH95 with tool A. when cutting speed *v*=35m/min, depth of cut a_p=0.9mm, feed *f*=0.02mm/z, cutting force was enormous in this experiment and the tool damaged. Thus, it can concluded that tool A is effective in cutting speed below 35m/min, it is unfit for machining FGH95 superalloy as cutting speed exceeds 35m/min. The primary goal of this text is

then to investigate the cutting temperature and cutting force in the end milling of FGH95 with AlTiN coated carbide end mill.

3.1.1 Influence of cutting speed on cutting forces

The speed range of machining tests was varied from 45 to 65m/min. Typical variation of cutting forces as cutting speed varies is shown in Fig.4.

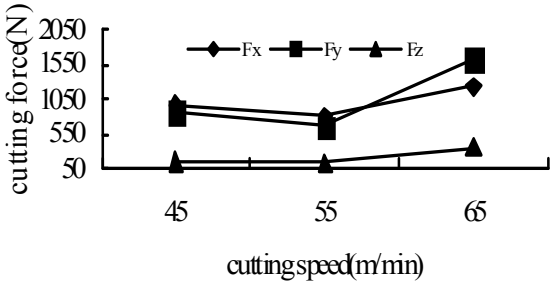

Figure4: Typical variation of machining forces with cutting speed

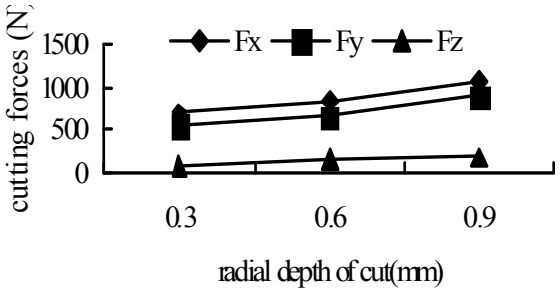

Figure5: Typical variation of cutting forces with radial depth of cut

It is seen from Fig.4 that after an initial decrease, the cutting force components rise in magnitude as the cutting speed increases. With lower cutting speed range from 45 to 55m/min, the cutting forces showed a somewhat reduce, but the reduce magnitude was quite small. This was due to in low cutting speed range, with the increasing of cutting speed, the fraction between tool and workpiece and the plastic deformation of materials raised, more heat generates from cutting zone. Workpiece material softening occurs. The force to separate chips from workpiece is thus grown down slightly. As the cutting speed further increases from 55 to 65m/min, fraction between tool and work-piece and the plastic deformation of materials sharply increased, which results in cutting forces explodes. From the Fig.5, it can be seen that the *Fx* and *Fy* component were greater than *Fz* by a considerable margin. This in conformity with the machining mode, there is no feed in axial direction (Z-direction).

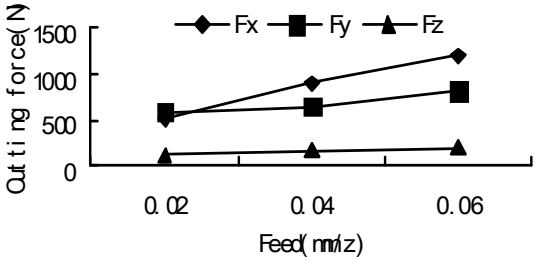

Figure 6: Typical variation of cutting forces with feed rate

3.1.2 Influence of radial depth of cut on cutting forces

The values of radial depth of cut varied from 0.3mm to 0.9mm. The variations of cutting forces with the radial depth of cut are shown in Fig.5. Except for *Fz*, other two cutting force components including *Fy* and *Fx* are seen to increase sharply with the radial depth of cut. This is due to the machining area size of cut per tooth increasing as the radial depth of cut increases. The cutting force component *Fx* dominates over the *Fy* and *Fz*.

3.1.3 Influence of feed per tooth on cutting forces

The feed per tooth of machining varied from 0.02 to 0.06mm/z.Typical variation of cutting forces with feed rate is shown in Fig.6. From Fig.6 it is observed that the cutting force components increase as the feed rate increases. The reason for

this increase of cutting force with the increase with the increase of feed rate is the load on each tooth increases as the feed increases. With the increase of feed rate, the cutting force component *Fx* increases faster than the *Fy* and *Fz*. The value of the *Fz* is smaller and has less variation.

3.2 Cutting temperature test

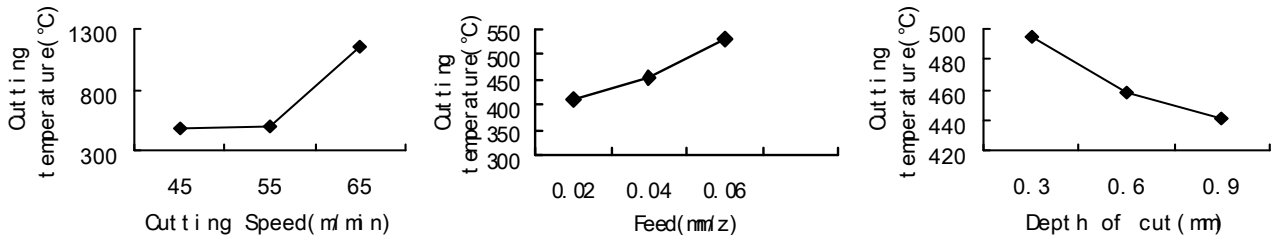

Figure 7: Influence of cutting parameters on cutting temperature

Under the same conditions stated above, the influence of cutting parameters (cutting speed (v), feed rate (f), radial depth of cut (a_p)) on cutting temperature when machining FGH95 superalloy by using tool B were studied. Portable thermal infrared radiation imager TH4105 was applied. The infrared emissivity was set 0.10[17]. The cutting temperature results during cutting test are shown in Fig.7. It can be seen from Fig.7 that the influence of cutting speed on cutting temperature is greatest. Temperature surge increases sharply as the cutting speed from 55m/min to 65m/min, the cutting temperature reaches to 1150℃, which lead the tool wears rapidly due to fast diffusers and strongly bonded between workpiece and tool materials. The feed rate and radial depth of cut has relatively low impact on cutting temperature.

However, cutting temperature decreases slightly with the radial depth of cut increases. This is due to with the radial depth of cut increased, the chip thickness increases, chip takes away more heat. The temperature on cutting area thus reduces slightly.

3.3 Tool wear mechanism

Tool wear mechanisms are generally influenced by three phenomena, namely thermal softening, diffusion and notching. Tool temperatures in tool body when machining nickel-based alloys are much higher than that when machining conventional steels [18]. Since nickel-based alloys work harden rapidly, once the milling cutter starts cutting, it will become more and more difficult for further machining due to hardening effect. When the cutting edge is not sharp enough, the metal is pushed instead of cut. This will result in higher cutting force and higher temperature. For the coated solid carbide end mill, although the coating layers can improve wear resistance significantly, it is still hard to bear the high load impacts and high temperature. Actually the coated layer cannot stand for long before it was worn [19]. There was a lot of strengthening phase and hard particles into the PM parts, which may cause abrasive wear. All factors mentioned above will result in severe tool wear and shorten tool life. The graphic of tool wear and breakage (Fig.8) showed that the dominant mechanism of tool wear was crater wear. Chipping damage was also observed on the flank surface, flank wear was quite limited.

3.4 Surface topography

The roughness for the surface of a machined product is important because of its effect on the general appearance. It has also more important technical effects. Many critical products, especially those required for aerospace purpose, must be machined to close tolerances of roughness as well as dimensions, and for items subject to fatigue the method of finishing may be specified [20].

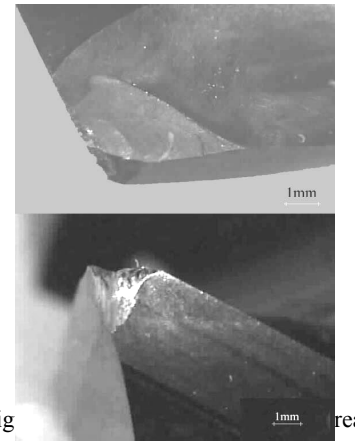

Fig reakage

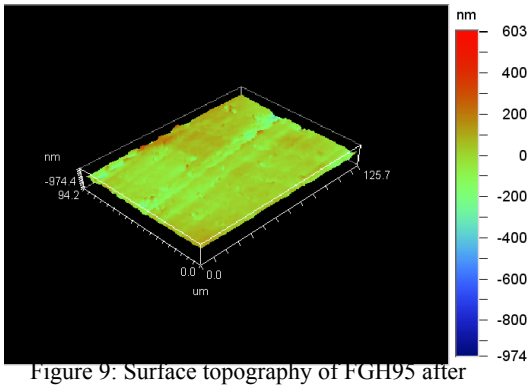

Figure 9: Surface topography of FGH95 after machining (v=45m/min, a_p=0.9mm, f=0.06mm/z)

Surface topography is conveniently described by division into two components [21]: including the geometric form or waviness resulting from the tool shape, feed rate or the other regular variables, and the roughness or random superimposed irregularities which are always present. The measurements of surface topography were carried out with white light interferometer and super depth field microscope. The machined surface topography of FGH95 with Tool B is shown in Fig. 9. As shown in Fig.9, the waviness is obviously under cutting speed is 45m/min, radial depth of cut is 0.9mm, and feed is 0.06mm/z. The roughness of surface Ra is 52.75nm.

4. CONCLUSIONS

The effect of cutting speed, radial depth of cut, and feed rate on machinability of FGH95 in end milling operation are investigated though experiments. Cutting forces, cutting temperatures, tool wear, and machined surface topography are analyzed. From the results obtained in the present work, the following conclusions can be drawn:

1. The cutting performance of end mill with AlTiN coating in machining FGH95 is better than that with TiAlN/TiN/TiAlN coatings.

2. With the increase of cutting speed, radial depth of cut, and feed, there is a growing tendency in cutting forces. Among them, cutting speed has the greatest influence on cutting forces, especially when cutting speed exceeds 55m/min.

3. With the increase of cutting speed and radial depth of cut, cutting temperature increases, while it decreases slightly as the increase of feed.

4. Chipping on cutting edge dominates in the tool wear mechanism, which is caused by porosity in FGH95 generating an interrupted cutting on microscopic scale.

5. Machined surface topography of FGH95 by using end mills with AlTiN coatings shows that it has better surface roughness and waviness than that with TiAlN/TiN/TiAlN coatings.

ACKNOWLEDGEMENTS

This work is supported by the National Natural Science Foundation of China (Grant No. 50828501 and 50935003), Foundation of Shandong Province of China for Distinguished Young Scholars (Grant No. JQ200918), National Basic Research Program of China (Grant No. 2009CB724401), and Mega-project of High-grade NC Machine Tools and Basic Manufacturing Equipment (Grant No. 2009ZX04014-043, 2009ZX04012-031 and 2009ZX04012-012).

REFERENCES

1. ZHANG Yi-wen, SHANGGUAN Yong-heng, Research and development in P/M superalloy [J], Powder Metallurgy Industry, vol.14 (6) pp.30-42,2004

2. GUO Wei-min, FENG Di, WU Jian-tao, et al. Research and development of P/M superalloy metallurgic Techniques [J], Material Engineering,vol.9 (3), pp. 44-48, 2002.

3. WANG Wu-xiang, MAO Jian, HU He, et al. As-HIP FGH95 powder metallurgy superalloy turbine disks [J], Material Engineering,(12), pp.39-43, 1999.

4. GUO Wei-min, FENG Di, ZHANG Feng-ge, WU Jian-tao, et al. Nickle-base PM superalloy FGH95 for discs [J], Journal of iron and steel research, vol.14 (3), pp.30-34, 2002.

5. S.M.Darwish, Machining of difficult-to-cut materials with bonded tool [J], International Journal of Adhesion & Adhesives, (20), pp.279-289, 2000.

6. A.Salak, K.Vasiko, M.Selecka, et al. New short time face turning method for testing the machinability of PM steels [J], Journal of Materials Processing Technology, (176), pp.62-69, 2006.

7. Etienne Robert-Perron, Carl Blais, Sylvaln Pelletier, et al. Machinability of green powder metallurgy components [J], Metallurgical and Materials Transactions, (38), pp.1330-1336, 2007.

8. I.A.Choudhury, M.A.EI-Baradie, Machinability of nickel-base superalloy: a general review [J], Journal of Materials Processing Technology, (77), pp.278-284, 1998.

9. Don Graham, Machining PM parts [J], Manufacturing Engineering, (6), pp.64-70, 1998.

10. L.Jiang, H.Hanninen, J.Paro, V.Kauppinen, Active wear and failure mechanisms of TiN coated high speed steel and TiN-coated cemented carbide tools when machining powder metallurgically made stainless steels [J], Metall. Trans, (27), pp.2796-2808,1996.

11. T.I.Elwardany, E.mohammed, M.A.Elaestawi, Cutting temperature of ceramic tools in high speed machining of difficult-to-cut materials [J], Pergamon, vol.36 (5), pp.611-634, 1996.

12. H.Chandrasekaran, J.Johansson, Chip flow and notch wear mechanisms during the machining of high austenitic stainless steels [J], Annals CIRP, (43), pp.101-105, 1994.

13. Jukka Paro, Hannu Hanninen, Veijo Kauppinen, Tool wear and machinability of HIPed P/M and conventional cast duplex stainless steels [J], Wear, (249), pp.279-284, 2001.

14. LI Xiao, ZHANG Maicang, ZHANG Lina, et al. Effect of inclusion on mechanical properties of powder metallurgical superalloy [J], Special Steel, vol.22 (1), pp.25-28, 2001.

15. ZHANG Shou-hua, HU Ben-fu, LI Hui-ying, et al. The microstructure and properties of a nickel base superalloy FGH95 [J], Journal of University of Science and Technology Beijing, vol.15 (1), pp.1-9, 1993.

16. GUO Wei-min, ZHANG Feng-ge, FENG Di, et al. Effects of producing process on microstructure and properties of FGH95 P/M superalloy [J], Powder Metallurgy Industry, vol.11 (5), pp.7-12, 2001.

17. HUANG Zhibin, ZHU Dongmei, LUO Fa, et al. High temperature oxidation behavior and infrared character of a Ni-Based superalloy K424 [J], Rare Metal Materials and Engineering, vol.37 (8), pp.1411-141, 2008.

18. E.F.Smat, E.M.Trent, Temperature distribution in tools used for cutting iron, titanium and nickel [J], Production. Research, vol.13 (3), pp.265-290, 1975

19. H.Z.Li, H.Zeng, X.Q.Chen, An experimental study of tool wear and cutting force variation in the end milling of Inconel 718 with coated carbide inserts [J]. Journal of Materials Processing Technology, (180), pp.296-304, 2006.

20. Kahles.J.F and Field M. Properties and Metrology of surface [M], Oxford, pp.31-45, 1968.

21. T.H.Childs, G.W.Rowe, Physics of metal cutting [M], pp.269-271, 1973.